Nanotechnology **21** (2010) 255704 (11pp) doi:10.1088/0957-4484/21/25/255704

Enhancement in the efficiency of polymerase chain reaction by TiO_2 nanoparticles: crucial role of enhanced thermal conductivity

Abdul Khaliq R[1,2], Parshuram J Sonawane[1], Binu K Sasi[1], Bhavani S Sahu[1], T Pradeep[3,4], Sarit K Das[2,4] and Nitish R Mahapatra[1,4]

[1] Department of Biotechnology, Indian Institute of Technology Madras, Chennai 600036, India
[2] Department of Mechanical Engineering, Indian Institute of Technology Madras, Chennai 600036, India
[3] Department of Chemistry, Indian Institute of Technology Madras, Chennai 600036, India

E-mail: pradeep@iitm.ac.in, skdas@iitm.ac.in and nmahapatra@iitm.ac.in

Received 19 April 2010, in final form 3 May 2010
Published 2 June 2010
Online at stacks.iop.org/Nano/21/255704

Abstract
Improvement of the specificity and efficiency of the polymerase chain reaction (PCR) by nanoparticles is an emerging area of research. We observed that TiO_2 nanoparticles of ~25 nm diameter caused significant enhancement of PCR efficiency for various types of templates (namely plasmid DNA, genomic DNA and complementary DNA). By a series of experiments, the optimal TiO_2 concentration was determined to be 0.4 nM, which resulted in up to a seven-fold increase in the amount of PCR product. As much as 50% reduction in overall reaction time (by reduction of the number of cycles and the time periods of cycles) was also achieved by utilizing TiO_2 nanoparticles without compromising the PCR yield. Investigations of the mechanism of such PCR enhancement by simulations using the 'Fluent K epsilon turbulent model' provided evidence of faster heat transfer in the presence of TiO_2 nanoparticles. Consistent with these findings, TiO_2 nanoparticles were observed to augment the denaturation of genomic DNA, indicating more efficient thermal conductivity through the reaction buffer. TiO_2 nanoparticle-assisted PCR may be useful for profound reduction of the overall PCR reaction period and for enhanced amplification of DNA amplicons from a variety of samples, including GC-rich templates that are often observed to yield unsatisfactory results.

(Some figures in this article are in colour only in the electronic version)

Nomenclature/abbreviations

C_p	specific heat (J kg^{-1} K^{-1})
k	thermal conductivity (W m^{-1} K^{-1})
T	temperature (°C)
μ	dynamic viscosity (N s m^{-2})
ρ	density (kg m^{-3})
φ	nanoparticle volume fraction
bf	base fluid
nf	nanofluid
p	particle
T_m	melting temperature of DNA (°C)

[4] Authors to whom any correspondence should be addressed.

1. Introduction

The polymerase chain reaction (PCR) is an *in vitro* DNA amplification process that serves as a powerful tool in numerous molecular biology applications, including direct cloning from

 © 2010 IOP Publishing Ltd Printed in the UK & the USA

genomic DNA or cDNA, site-directed mutagenesis, genetic fingerprinting for forensic analysis, medical diagnostics and analysis of allelic sequence variations [1]. However, it is well known that primer–dimer formation, high GC% of the template DNA and sub-optimal heating/cooling ratio of the thermocycler interfere with the PCR efficiency and specificity. Therefore, there is a need to improve the specificity and efficiency of this widely used molecular biology technique. Besides some commercial enhancers of unknown composition, several reagents (namely betaine, dimethyl sulfoxide, dithiothreitol, formamide and glycerol) are used as PCR additives on a trial-and-error basis for this purpose [2–6]. The efficiency of PCR has also been improved by developing thermocycler machines capable of rapid heating–cooling (6–9 °C s^{-1} or more) responses.

Nanoparticles are novel materials that have many physical properties different from larger-sized materials, enabling their applications in biological research [7]. Notably, the thermal efficiency of nanoparticles has been reported to be enhanced with decreasing size of the particles [8–10]. Furthermore, several studies by ourselves and others have showed that nanoparticles significantly increase the thermal conductivity of fluids over a volume fraction range of 0.1%–5.0% [11–18]. It has also been reported that nanoparticles can transport heat flux and cause thermal equilibrium with the environment within 10–200 ps in liquid [16]. In view of the above observations, nanoparticles seem to be attractive modulators of PCR by virtue of their efficient heat transfer property. Indeed, gold nanoparticles have been shown to significantly improve both the specificity and sensitivity of PCR reactions [19]. Additionally, tetrapod-like ZnO nanostructures, single-walled carbon nanotubes and carbon nanopowder were found to increase PCR efficiency and specificity [20, 21]. Thus, nanoparticle-assisted PCR is an emerging area of research that may enhance the specificity and efficiency of PCR amplification of target DNA.

Although an enhanced heat transfer effect due to nanoparticles is thought to be involved in this phenomenon, little is known regarding the exact mechanism behind the PCR improvement by nanoparticles. In this study, we have tested the effect of inexpensive TiO_2 nanoparticles (that reportedly display up to 33% enhancement of thermal conductivity for 5% volumetric loading [22]) on PCR efficiency using gene-specific primers to amplify DNA segments of various sizes from a variety of templates, including GC-rich promoter regions from human genomic DNA. Significant enhancement of PCR yield and a profound reduction of the overall cycling time were achieved by TiO_2 nanofluids. We also investigated the underlying mechanism of these effects by computational modeling of the potential enhancement of heat transfer by TiO_2 particles and by the experimental determination of template DNA denaturation efficiency in the presence or absence of these nanoparticles. This study shows that TiO_2 nanoparticles indeed cause a rapid increase in thermal conductivity of the fluid and thereby contribute to the enhancement of PCR efficiency.

2. Materials and methods

2.1. Preparation of TiO_2 nanofluids

TiO_2 nanoparticles of ∼25 nm (Sigma-Aldrich, USA) were suspended in molecular biology-grade sterile water (Hi-Media, India) at 10 mM concentration. To ensure proper mixing of the nanoparticles in water, sonication was performed for 30 min using bath-sonicator equipment (37 ± 3 kHz, 150 W; TOSHCON Ultrasonic Cleaner, TPI Pvt. Ltd). This well dispersed nanofluid was used as a stock solution and was appropriately diluted to various concentrations (0.2–3.2 nM) in the PCR reaction mixtures. Concentrations (in terms of the particles) were calculated using the average particle size and the bulk density of TiO_2. The pH of the stock nanofluid was 4.8 ± 0.05 and was a clear transparent fluid.

2.2. Transmission electron microscopy (TEM)

For physical characterization of the TiO_2 nanoparticles suspended in sterile water, transmission electron microscopy was performed. TEM measurements of all the samples were done after they were drop-casted onto a carbon-coated copper grid and dried in ambient conditions with a JEM 3011 (JEOL Ltd) 300 kV high-resolution transmission electron microscope (HRTEM) with a UHR polepiece.

2.3. DNA templates

We have used a variety of templates (namely mouse and human genomic DNA, plasmid DNA and mouse complementary DNA [cDNA]) in this study. The mouse genomic DNA samples used in this study were obtained from the Jackson Laboratory, USA. The human genomic DNA was isolated from blood samples of healthy volunteers (following a protocol approved by the institutional ethics committee) using a Flexigene DNA isolation kit (Qiagen).

The plasmid DNA was isolated by an alkaline lysis method. In brief, 12 ml of Luria Broth containing ampicillin was inoculated with *E. coli* DH5α (harboring human MAO-C promoter-luciferase reporter plasmid) and incubated overnight at 37 °C with shaking at 200 rpm. The cells were pelleted down at 12 000 rpm and re-suspended in 600 μl ice-cold solution I (50 mM glucose, 25 mM Tris-Cl (pH 8.0), 10 mM EDTA (pH 8.0), supplemented with 25 μg ml^{-1} RNase), then lysed with 1.2 ml of solution II (0.2 N NaOH, 1% SDS) for 5 min, followed by addition of 900 μl of solution III (3 M sodium acetate, pH 5.2–5.4) and incubation on ice for 10 min. The tubes were then centrifuged at 12 000 rpm for 5 min and the supernatants were collected in fresh tubes. Approximately three volumes of chaotropic salt solution and 60 μl of glass powder suspension (Hi-Media, India) were added to the supernatants, followed by incubation for 10 min and centrifugation at 12 000 rpm for 2 min. The pellets thus obtained were washed three times with the washing buffer (Hi-Media, India) and the plasmid DNA was eluted in water by incubating at 55 °C for 10 min. Tubes were centrifuged for 2 min at 12 000 rpm to collect the plasmid DNA.

Table 1. Oligonucleotide primers used for PCR amplifications.

Target gene and location (NCBI Acc. No.)	Forward primer: sequence, GC content, Tm	Reverse primer: sequence, GC content, Tm	Amplicon size and GC content
Mouse HMGCR, Exon 11 (NM_008255)	mHMGCR11982-FP: 5′-CCGTGCTGTGTTCTTCATCTCAG-3′; 52.2%; 56.3 °C	mHMGCR 12345-RP: 5′-TCCTCTGTATTCTCCCCCAGTGTG-3′; 54.2%; 58.1 °C	364 bp; 51.9%
Human MAO-C promoter (NM_001031709)	hRen375-FP: 5′-CGGGGTACCCCA ACAGGCATGAGAGTTATCG-3′; 58.06%; 72.13 °C	hRen19-RP: 5′-CCGCTCGAGAGA GGGAGCAGCGATCCG-3′; 70%; 74.10 °C	394 bp; 65%
Human CHGA, Exon 7 (NM_001275)	hCHGA9236-FP: 5′-CCCATTCTCCTGCTCTTGCC-3′; 60.0%; 56.0 °C	hCHGA 9769: 5′-TCCCGCCCCATACCAACCTC-3′; 65.0%; 60.3 °C	534 bp; 66.3%
Human HSPA1A promoter (NM_005345)	hHSP947-FP: 5′-CGGGGTACCTAT CCCTCTCCACACCGCAGATTC-3′; 60.60%; 74.45 °C	hHSP88-RP: 5′-CCGCTCGAGCGG GAGTCACTCTCGAAAAAGGTAG-3′; 58.82%; 74.30 °C	1035 bp; 60.1%
Mouse HMGCR, cDNA domain between Exon 9 and Exon 11 (NM_008255)	mHMGCR 11481-FP: 5′-TTGGTCCTTGTTCACGCTCATAG-3′; 47.8%; 55.8 °C	mHMGCR 12138-RP: 5′-CTCTGCTTGTAGTCTCTGCTTCCAC-3′; 52.0%; 55.6 °C	448 bp; 46%

The mouse cDNA was prepared from the total RNA extracted from mouse liver (obtained from the Jackson Laboratories, USA) using Trizol reagent (Invitrogen, USA), SuperscriptIII™ reverse transcriptase (Invitrogen, USA) and random hexamer oligonucleotides following the manufacturer's protocol.

Concentrations of the templates were ascertained by UV-spectroscopic measurements. The DNA samples were diluted to 20 ng μl^{-1} in water and stored at 4 °C until use in PCR.

2.4. PCR methodologies

PCR was carried out to amplify a range of different segments of genomic DNA using gene-specific primers (table 1) synthesized from Ocimum Biosolutions (India). Optimization and amplification of these DNA segments were performed using Taq DNA polymerase, ThermoPol buffer and dNTPs from the New England Biolabs, USA. The typical PCR reaction mixture contained the following final concentrations: 1.5 mM $MgCl_2$, 0.4 mM each dNTP, and 1 μM of each forward/reverse primer and 10–20 ng of template DNA per 20 μl reaction with or without different concentrations (0.1–3.2 nM) of nanoparticles. In some experiments, we used a lower concentration (0.25 μM) of primers and different concentrations of templates (from as high as 40 ng μl^{-1} to as low as 0.625 ng μl^{-1}). The PCR protocol began with a 94 °C denaturation step for 5 min, followed by a Touchdown program (94 °C denaturing step for 30 s followed by initial annealing temperature of 70 °C, subsequently run down to 55 °C at 1 °C/cycle, and a 72 °C extension step for 1 min), followed by a uniform three-step amplification profile (94 °C denaturing step for 30 s, 54 °C annealing step for 30 s, 72 °C extension step for 1 min) for another 23 cycles, then 72 °C for 10 min, and finally held at 4 °C as described previously [23]. In some experiments, we reduced the times of denaturation, annealing as well as amplification by up to 50% of the above mentioned times. In another set of experiments, we gradually reduced the number of cycles in the uniform three-step segment of the above mentioned PCR program while keeping the cycling times constant. For example, we first reduced the number of cycles from 23 to 19, and then to 18. The PCR reactions were carried out using a thermocycler with maximum ramping rate of 2.5 °C s^{-1} (Model PTC-1148; Bio-Rad). After PCR, the products were run in agarose gels (1.2% wt/vol (in the case of smaller amplicon) or 1.0%, wt/vol (in the case of larger amplicon)) and visualized by ethidium bromide staining.

2.5. Quantitative estimation of amplified PCR products

The amounts of amplified PCR products were quantified by three different techniques. Firstly, NIH Image J software was used for densitometric scanning of the gel pictures generated by loading an equal volume of PCR products. The band intensities were expressed as arbitrary units (a.u.). Secondly, DNA concentrations of the PCR products were determined by the measurement of absorbance at 260 nm. For this purpose, 5.0 μl of PCR product from each of the conditions (including the PCR negative control in which no template was added) was treated with Exo-SAP enzyme cocktail (containing 0.15 μl of exonuclease–1 (20 U μl^{-1}; Fermentas, USA), 0.80 μl Shrimp Alkaline phosphotase (1 U μl^{-1}; Fermentas, USA) and 2.9 μl H_2O) and incubated at 37 °C for 45 min to degrade the unutilized dNTPs and primers. Two different volumes (2.5 and 5.0 μl) of these Exo-SAP treated samples were subjected to DNA estimation by UV spectroscopy for accuracy. Fold increases in the nanoparticle-added PCR samples with respect to the positive control PCR (in which no nanoparticle was added) were calculated to determine the effect of TiO_2 nanoparticles. Thirdly, we also carried out quantitative estimation of gel-purified (using a chaotropic salt–

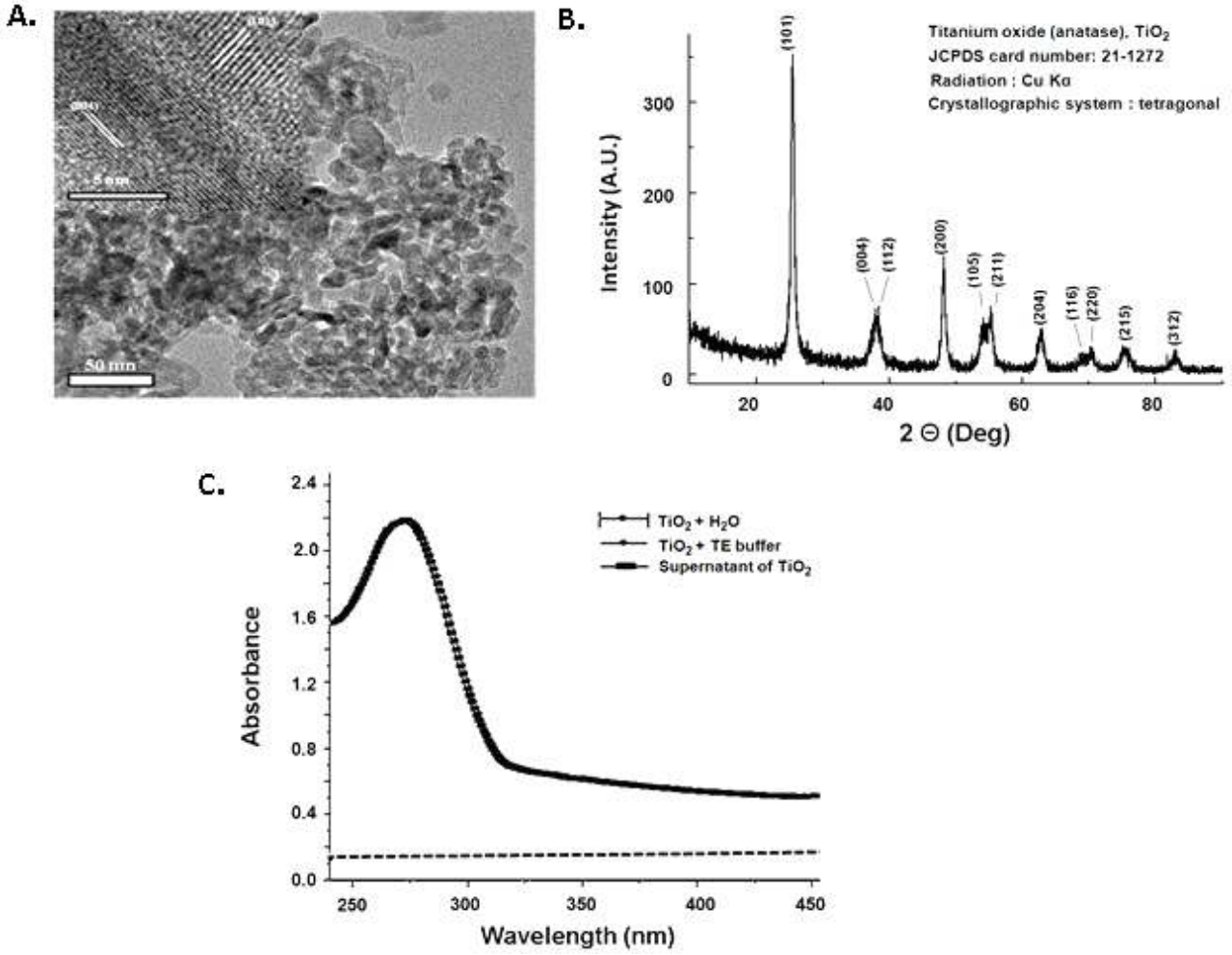

Figure 1. Physical characterization of TiO_2 nanoparticles. (A) Lattice resolved transmission electron microscopy (TEM) image of TiO_2 nanoparticles suspended in water (inset). The average diameter was 25 nm and the spacing between lattices were 0.35 nm for the (101) plane and 0.23 nm for the (004) plane. A large area image is given as the main figure. (B) X-ray diffraction analysis of TiO_2 (anatase) nanoparticles. X-ray diffraction data were collected with a Bruker AXS D8 ADVANCE x-ray diffractometer using Cu Kα ($\lambda = 1.54$ Å) radiation. The samples were scanned in the 2θ range of 10°–90° and all of the peaks were assigned and compared with the database published by the Joint Committee on Power Diffraction Standards (JCPDS). The peak values were consistent with the *d*-spacings of the lattice resolved TEM image. (C) UV–visible spectroscopic observation of TiO_2 nanofluids (at 5 mM concentration) with water and TE buffer as base fluids. Both samples displayed a peak at 270 nm.

silica based kit, Hi-Media, India) PCR products in some cases to verify the efficacy of the Exo-SAP technique.

2.6. Evaluation of DNA denaturation by UV spectroscopy

Thermal denaturation experiments of DNA were conducted in a Perkin-Elmer Lambda 35 spectrophotometer by measuring the absorbance at 260 nm. The temperature (35–95 °C) was controlled by a Peltier system (±0.1 °C). The measurements were done using Herring Sperm DNA (Hi-Media, India) in water in duplicates. Two different concentrations (12.5 and 25 μg ml^{-1}) of the DNA solution were tested to ensure accuracy in the absorbance values. The thermal denaturation experiments were carried out in the presence and absence of TiO_2 nanoparticles to determine the effect of nanoparticles on the DNA denaturation.

3. Results and discussion

3.1. Physical characterization of the TiO_2 nanoparticles

Analysis of the TiO_2 nanoparticles by TEM showed the average diameter to be 25 nm (figure 1(A)). The particle size distribution confirmed that most of the nanoparticles are within the range of mean diameter (25 ± 10 nm). Lattice resolved TEM imagery showed that the TiO_2 nanoparticles were in the anatase phase with a spacing of 0.35 nm for the (101) plane and 0.23 nm for the (004) plane (figure 1(A)). The *d*-spacings observed in TEM were confirmed by x-ray diffraction analysis (figure 1(B)). Analysis of UV–visible absorption spectra of TiO_2 nanoparticles (suspended in water) showed a peak at 270 nm (figure 1(C)). No difference in the spectrum was observed when TE buffer (10 mM Tris, 1 mM EDTA, pH 8.0) was used instead of water as the base fluid. The peak was detectable in the concentration range of 1–10 mM. In

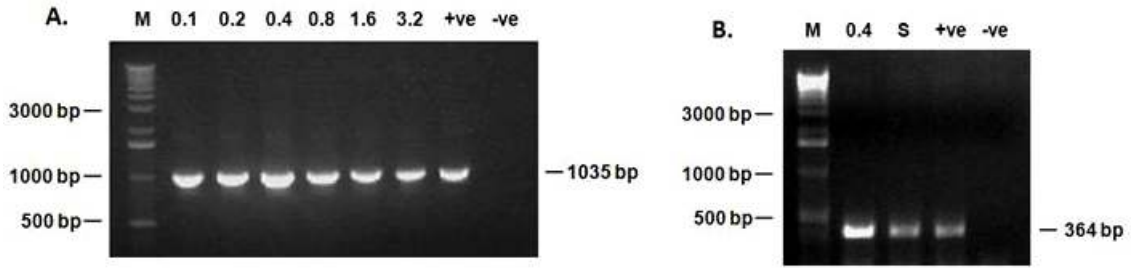

Figure 2. (A) Agarose gel electrophoresis of PCR products showing concentration-dependent effect of TiO_2 nanoparticles. PCR amplification of a 1035 bp region of human HSPA1A promoter was carried out in the presence of 0.1–3.2 nM TiO_2 nanoparticles. The lane labeled as '+ve' indicate the PCR products obtained under identical conditions without addition of the nanoparticles and the lane labeled as '−ve' indicates the negative control reaction in which water was added instead of template DNA. The lane labeled as 'M' shows positions of the DNA molecular weight markers. (B) Agarose gel electrophoresis of PCR products showing TiO_2 nanoparticle-specific augmentation of PCR yield. The lane labeled as '0.4' indicates the PCR product obtained in the presence of 0.4 nM TiO_2 nanoparticles; the lane labeled as 'S' indicates the PCR amplified product using the supernatant of TiO_2 nanoparticle suspension. 'M', '+ve' and '−ve': same as mentioned above.

order to ensure that the peak at 270 nm is specific to the TiO_2 nanoparticles, we centrifuged the aqueous suspension and measured the absorbance of the supernatant, which did not display any peak in the entire spectral window (figure 1(C)).

3.2. TiO_2 nanoparticles increase PCR yield

To test the effect of TiO_2 nanoparticles on PCR yield we used several gene-specific oligonucleotide primers (table 1) for amplification of a variety of amplicons (namely different sizes, different GC content) and different types of template DNA samples (namely plasmid DNA, mouse and human genomic DNA and mouse cDNA) in the presence of different concentrations (0.1–3.2 nM) of nanoparticles. Repeated experiments with different templates and primers showed that TiO_2 nanoparticles increased the PCR yield in a concentration-dependent manner, with maximal augmentation at 0.4 nM. For example, figure 2(A) shows maximal amplification of a 1035 bp Hspa1a promoter DNA fragment from the human genomic DNA in the presence of 0.4 nM TiO_2 nanoparticles. As a negative control for PCR, we carried out a reaction without any template, which did not yield any product (figure 2).

In order to confirm that the enhancement of PCR yield was specifically caused by TiO_2 nanoparticles and not by any impurities (additives or surfactants, which may be present in the commercially purchased nanoparticles), we carried out experiments with the supernatant of TiO_2 suspension devoid of TiO_2 nanoparticles. The supernatant was obtained after centrifugation of freshly prepared TiO_2 nanofluids at 12 000 rpm for 30 min. No PCR enhancement was observed when an equal volume of supernatant was used instead of TiO_2 nanofluids in the PCR reagent mixture in repeated experiments. For example, augmentation in the yield of a 364 bp DNA segment of mouse HMG-CoA reductase gene was observed in the presence of 0.4 nM TiO_2, while the nanofluid supernatant (that may contain any surfactant or ion part of the nanoparticle system) did not display any effect (figure 2(B)).

To quantitatively determine the extent of PCR enhancement in the presence of TiO_2 nanoparticles, we measured the amount of PCR products by different techniques, as described in section 2. We estimated that 0.4 nM TiO_2 nanoparticles resulted in an ∼2.9-fold enhancement of the 364 bp DNA amplicon from mouse genomic DNA (figure 3(A)) as well as ∼3.6-fold and ∼3.0-fold enhancements of 534 bp and 1035 DNA segments (figures 3(B) and (C)) respectively from human genomic DNA. Likewise, addition of 0.4 nM TiO_2 nanoparticles into the PCR reaction mixture also led to a profound increase (up to ∼7-fold) in the amplification of a 448 bp cDNA fragment of mouse HMG-CoA reductase gene (figure 4). Augmented amplification of these DNA amplicons of various sizes (from 364 to 1035 bp) reflects the robustness of these nanoparticles. Interestingly, TiO_2 nanoparticles resulted in the higher fold increases over the control (without nanoparticles) with a lower amount of template cDNA (figure 4), indicating that the lower limit of the amount of template in PCR can be significantly reduced by addition of 0.4 nM TiO_2 nanoparticles into the reaction mixture.

Notably, three of the amplicons included in this study contained highly GC-rich sequences (namely the 394 bp human MAO-C promoter, the 534 bp human CHGA exon seven segment and the 1035 bp human Hspa1a having 65%, 66.3% and 60.1% GC content respectively; table 1) that are often observed to give unsatisfactory results under standard PCR conditions. Robust amplifications of those difficult-to-amplify DNA segments clearly suggested the efficacy of the TiO_2 nanoparticles in PCR improvement.

3.3. TiO_2 nanoparticles enable reduction of reaction times

To further test the efficacy of the TiO_2 nanoparticles, we carried out the PCR reactions with a reduced number of cycles. As described in section 2, keeping the 'touch-down' part of the PCR program unchanged, we reduced the 'uniform three-step' number of cycles from 23 to 18. We amplified a 394 bp Human MAO-C promoter DNA segment using MAO-C promoter plasmid as the template. Similar to PCR reactions involving the regular 23 cycles, maximal amplification in the case of 18 cycles was also observed with 0.4 nM TiO_2

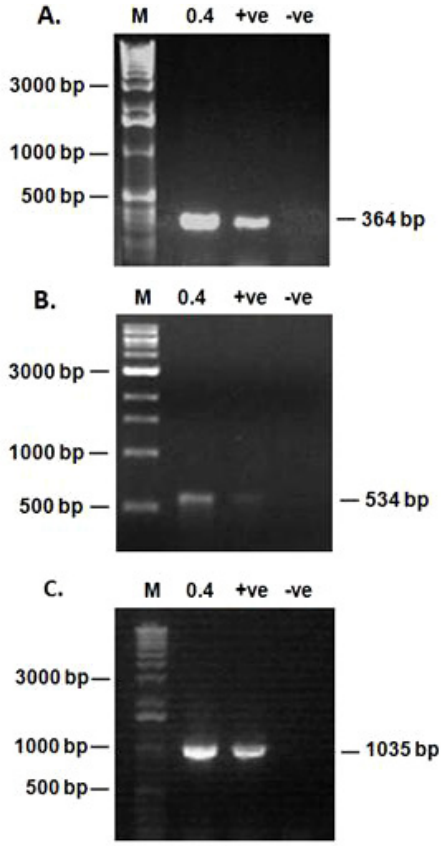

Figure 3. Agarose gel pictures of PCR products displaying enhancements in the yield in the presence of TiO_2 nanoparticles. Each of these experiments was repeated at least three times and representative pictures are shown. The lanes labeled as '0.4' indicate the PCR products obtained in the presence of 0.4 nM TiO_2 nanoparticles; the lanes labeled as '+ve' indicate the PCR products obtained under identical conditions without addition of the nanoparticles and the lanes labeled as '−ve' indicates the negative control reactions in which water was added instead of template DNA. (A) Amplification of 364 bp DNA segment of mouse HMG-CoA reductase (HMGCR) gene showing an ∼2.9-fold enhancement in the presence of TiO_2 nanoparticles. (B) Amplification of a GC-rich 534 bp DNA segment of human chromogranin A (CHGA) gene showing an ∼ 3.6-fold enhancement in the presence of TiO_2 nanoparticles. (C) Amplification of a GC-rich 1035 bp DNA region of human HSPA1A promoter. In the presence of TiO_2 nanoparticles, an ∼3.0-fold enhancement in the PCR yield was observed. The lanes labeled as 'M' show molecular weight marker positions.

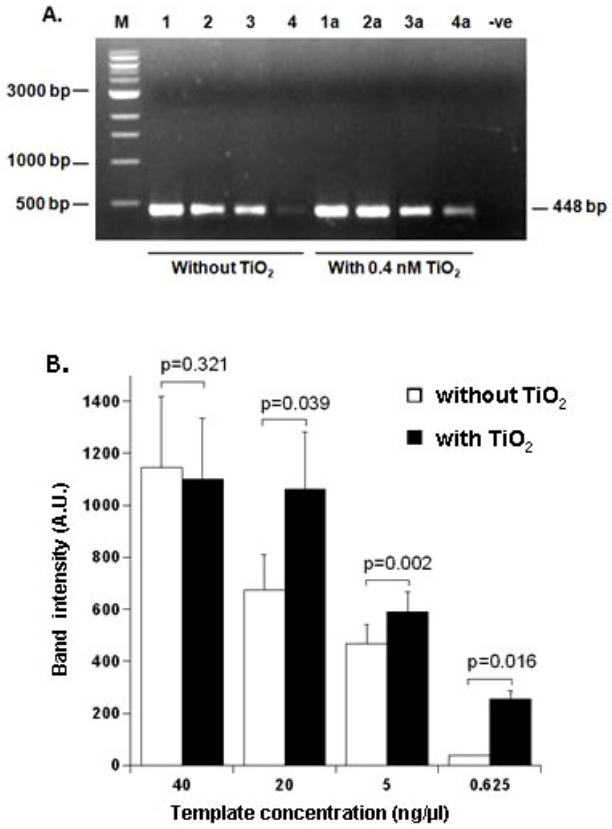

Figure 4. Template-dependent PCR amplification in the presence of TiO_2 nanoparticles. (A) Representative agarose gel picture showing amplification of a 448 bp DNA fragment by PCR using different concentrations of mouse cDNA templates in the absence or presence of 0.4 nM TiO_2 nanoparticles. Lanes from left: M, DNA molecular weight marker; 1 and 1a: 40 ng μl^{-1}; 2 and 2a: 20 ng μl^{-1}; 3 and 3a: 5 ng μl^{-1}; 4 and 4a: 0.625 ng μl^{-1}; −ve, negative control (without template cDNA). (B) Quantitative estimation of relative amounts of PCR yields. Although addition of TiO_2 nanoparticles did not show any effect in the case of high template concentration (40 ng μl^{-1}), lower template concentrations displayed a significant ($p < 0.05$) enhancement in PCR product. For example, ∼7.0-fold augmentation was observed in the case of the least template concentration (0.625 ng μl^{-1}). A.U.: arbitrary unit.

nanoparticles (figure 5(A)). Moreover, at this concentration of TiO_2 nanoparticles, reduction of the number of cycles from 23 to 18 did not cause any decrease in the amount of amplified product as compared to the control reaction (without nanoparticles) with 23 cycles, suggesting that as many as 5 cycles can be reduced in the PCR program without compromising with the amount of product through the addition of 0.4 nM TiO_2 nanoparticles in the reaction mixture.

We also investigated whether reduction of the denaturation, annealing and extension times in each cycle of the PCR can be achieved with the help of TiO_2 nanoparticles. Interestingly, even 50% reduction of time in each of these steps resulted in substantial amplification of the 364 bp mouse HMG-CoA reductase DNA amplicon in the presence of 0.4 nM TiO_2 nanoparticles in the reagent mixture. On the other hand, the extent of amplification in the absence of the nanoparticles was significantly (∼1.7-fold) lower (figure 5(B)), suggesting that the overall reaction time can be drastically reduced without compromising the PCR yield by utilization of the TiO_2 nanoparticles in the PCR.

3.4. Simulation of TiO_2 nanoparticle-assisted PCR

In order to investigate whether the mechanism of PCR enhancement by TiO_2 nanoparticles involves enhanced thermal conductivity of nanofluids, we developed a three-dimensional model, simulated with the Fluent software (that utilizes Fluent K epsilon turbulent model), to study the heat transfer contours with and without nanoparticles. The geometry of the typical PCR reaction tube used in this study with 0.2 mm thickness, 20 mm height and 0.2 ml volume was generated using

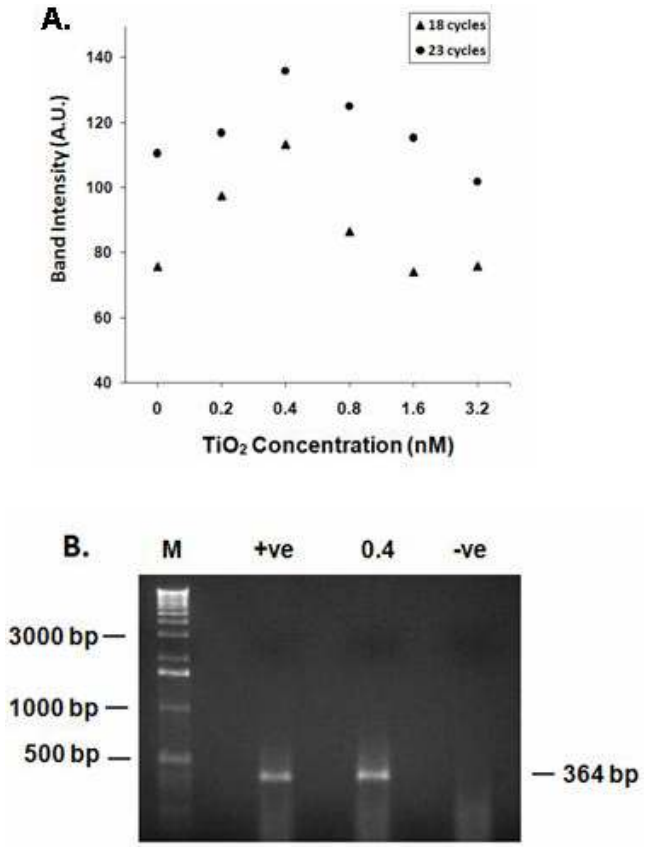

Figure 5. Effect of reduction of PCR reaction times. (A) Amplification of a 394 bp human MAO-C promoter DNA segment was carried out in the presence and absence of 0.2–3.2 nM TiO_2 nanoparticles with the regular number of cycles (23 cycles) and a reduced number of PCR cycles (18 cycles) as described in section 2. A.U.: arbitrary unit. (B) PCR amplification of a 364 bp mouse HMG-CoA reductase gene fragment after 50% time reduction in each step (denaturation, annealing and extension) of PCR cycles was carried out in the presence or absence of 0.4 nM TiO_2 nanoparticles, as described in the Materials and Methods section. Lanes from left: M, DNA molecular weight marker; +ve, positive control (without TiO_2 nanoparticles); −ve, negative control (without template DNA).

SolidWorks software (version 2006) and structured meshing was performed (figure 6(A)). The top surface was made adiabatic and the boundary conditions were determined in accordance with the actual PCR conditions. Three distinct points at 12 mm, 14 mm and 16 mm height, respectively, were placed along the axis of the tube to detect the temperature changes. Case-1 (without nanoparticles) was simulated with water as the base fluid (using the following values: $\rho = 998.2\ \mathrm{kg\,m^{-3}}$; $C_p = 4182\ \mathrm{J\,kg^{-1}\,k}$; $k = 0.6\ \mathrm{w\,mK^{-1}}$; $\mu = 0.001\,003\ \mathrm{kg\,ms^{-1}}$). In case-2 (with TiO_2 nanoparticles), the density of the nanofluid was calculated as $\rho_{\mathrm{nf}} = (1-\varphi)\rho_{\mathrm{bf}} + \varphi\rho_{\mathrm{p}}$ and the viscosity was expressed using Einstein's model as $\mu_{\mathrm{nf}} = \mu_{\mathrm{bf}}(1 + 2.5\varphi)$, whereas the effective thermal conductivity was determined, based on the Hamilton–Crosser model, as

$$K_{\mathrm{eff,Maxwell}} = \frac{K_{\mathrm{p}} + 2K_{\mathrm{l}} + 2(K_{\mathrm{p}} - K_{\mathrm{l}})\varphi}{K_{\mathrm{p}} + 2K_{\mathrm{l}} - (K_{\mathrm{p}} - K_{\mathrm{l}})\varphi} K_{\mathrm{l}}.$$

The specific heat was calculated using the Bergman equation on a mass-averaged expression as below:

$$C_{p,\mathrm{nf}} = \frac{\varphi(\rho c_p) + (1-\varphi)(\rho c_p)_{\mathrm{bf}}}{\varphi\rho_{\mathrm{p}} + (1-\varphi)\rho_{\mathrm{bf}}}.$$

For 30 time steps of 1 s each, the simulation was carried out and the transient regions of various temperature levels were analyzed in order to distinguish the two cases (figure 6(B)). The contours obtained were able to make a distinction between case-1 and case-2. Notably, the heat transfer measurements of the model with nanoparticles incorporated in it (figure 7) were identical with several temperature and particle volume fraction based nanofluid models [14, 17, 18]. Plotting time steps along the x-axis and the temperature (K) transferred from the walls of the tube along the y-axis with the observed data at the second point clearly showed that there was a sudden rise in temperature within a short span of time itself in the presence of nanoparticles, reaching saturation after time step 5, thus proving the effect of enhanced heat transfer due to nanoparticles (figures 6(B) and 7). The simulated results were consistent with our experimental findings that the desired PCR products were obtained with a considerably reduced number of cycles or with a reduced reaction time in each of the three steps in every cycle (figure 5).

3.5. TiO_2 nanoparticles augment DNA denaturation

In view of the above PCR simulation results suggesting efficient heat transfer by TiO_2 nanoparticles (figures 6 and 7), we asked whether these nanoparticles enhance denaturation of DNA, which is the first step in the PCR process. To monitor the extent of DNA denaturation, we measured the absorbance of genomic DNA solutions at 260 nm at various temperatures, as described in section 2. TiO_2 nanoparticles resulted in higher absorbance at 260 nm values than the control (without nanoparticles) over all the tested temperature range (from 35 to 95 °C) in two different concentrations (25 and 12.5 $\mu\mathrm{g\ ml^{-1}}$) of DNA solutions, indicating augmentation of DNA denaturation by the nanoparticles. As shown in the case of the 25 $\mu\mathrm{g\ ml^{-1}}$ genomic DNA solution containing the nanoparticles, the absorbance at 95 °C was ∼2.0-fold higher than the control DNA solution (figure 8). It is also noteworthy that TiO_2 nanoparticles seem to initiate the denaturation process even at temperatures as low as 35 °C (figure 8). Interestingly, the nanoparticles seem to exert their effect in a concentration-dependent manner, with the higher concentration (3 nM) of these nanoparticles yielding greater values than the lower concentration (2 nM) at all the tested temperatures (figure 8), indicating the necessity of an optimal TiO_2 concentration for the maximal heat transfer effect. It is important to note that the absorbance at 260 nm of TiO_2 was insignificant in these concentrations to contribute to the observed increase (figure 8).

3.6. Excess TiO_2 nanoparticle concentrations exert PCR inhibitory effect

Several parametric effects on nanofluid thermal conductivity enhancement include particle volume concentration, particle

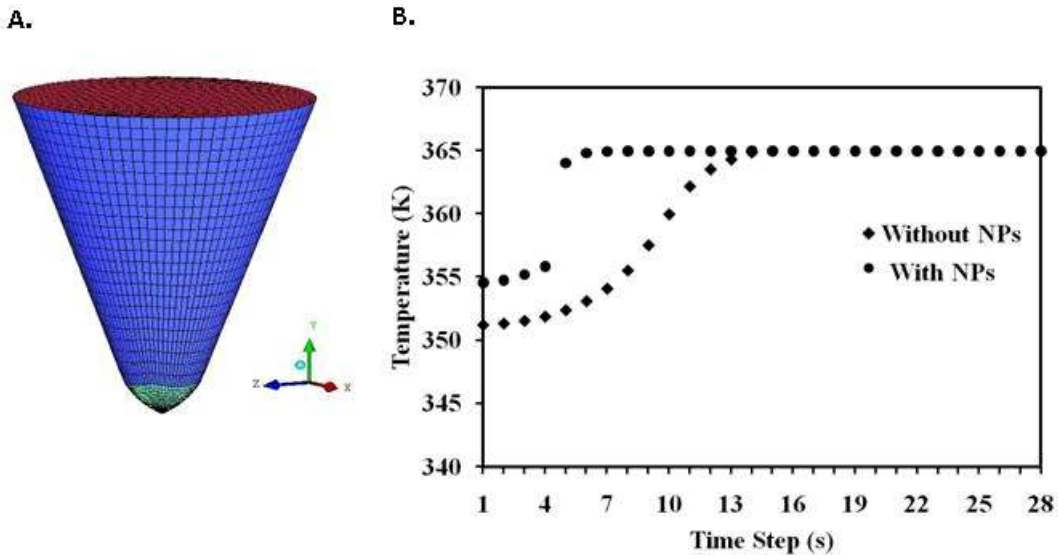

Figure 6. (A) Geometry of the simulated model for the conventional PCR tube of 20 mm height and 0.2 ml volume using SolidWorks software. The top surface being adiabatic, the tube has three points at (at 12, 14 and 16 mm) along its axial length to sense the temperature change. (B) Temperature recorded at point-2 during the simulation in the model using Fluent Software. A sudden rise of temperature in the presence of nanoparticles can be seen after 4 s.

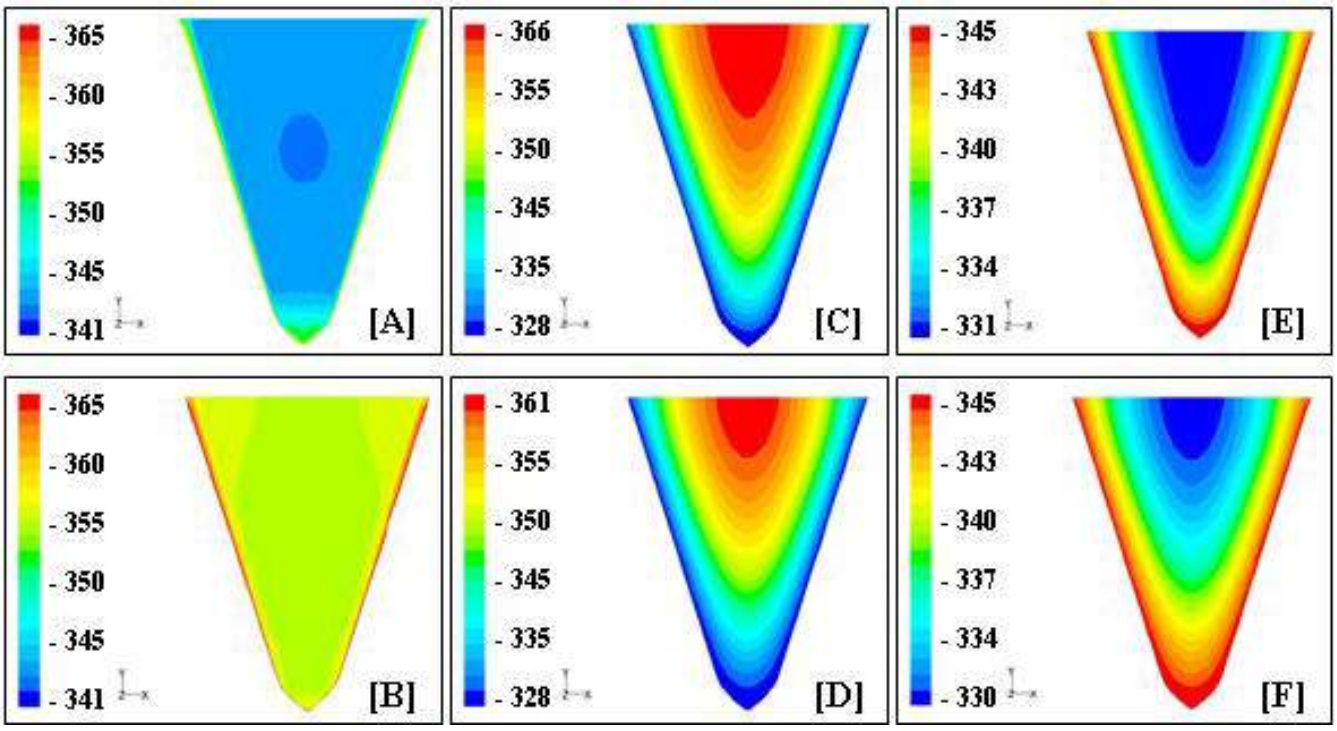

Figure 7. Temperature contours of the simulated model with three different PCR steps (denaturation, annealing and extension) using the Fluent software. *Top panel* (without TiO_2 nanoparticles): 28 °C–92 °C (A); 92 °C–55 °C (C); 55 °C–72 °C (E). *Bottom panel* (with TiO_2 nanoparticles): 28 °C–92 °C (B); 92 °C–55 °C (D); 55 °C–72 °C (F).

material, particle size, particle shape, base fluid material, temperature, additive, and acidity [24]. Though effects of all these parameters were not studied separately in the present PCR experiments, we found that temperature and nanoparticle concentration strongly influence the viability of reaction. It is conceivable that when the temperature during the denaturation steps in nanoparticle-assisted PCR goes above 363 K, the enhanced thermal conductivity effect [14] may degrade DNA due to higher heat conduction, resulting in an inhibition of PCR. Indeed, as shown in figures 2 and 5, the PCR-enhancing effect of TiO_2 nanoparticles displayed a dose-dependent pattern, and increasing the concentration in

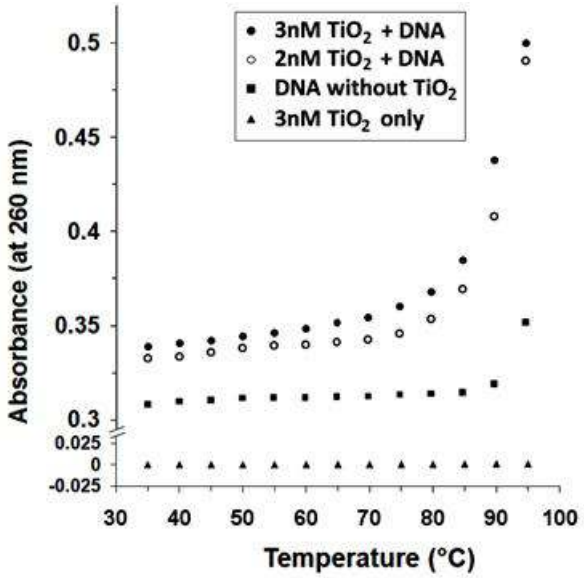

Figure 8. UV-spectroscopic observations of DNA denaturation with increasing temperature (from 35 to 95 °C) and TiO_2 nanoparticle concentrations (2 and 3 nM), as described in section 2. The measurements were done using 25 μg ml^{-1} genomic DNA in water in duplicates and the mean values were plotted against the corresponding temperature.

the reaction mixture beyond 0.4 nM resulted in the gradual loss of the enhancing effect. This is consistent with a previous report [25] that documented PCR inhibition at higher concentration (30–900 μg ml^{-1} = 370 nM–11.2 mM) of TiO_2 nanoparticles.

3.7. Effect of rutile TiO_2 nanoparticles on PCR efficiency

In order to test whether the enhancement of PCR efficiency by TiO_2 nanoparticles is dependent on the different polymorphic phases of TiO_2 molecules, we carried out PCR experiments using similar sized rutile TiO_2 nanoparticles. Experiments with different templates and primers showed that rutile nanoparticles increased the PCR yield at 0.4 and 0.8 nM concentrations. For example, figure 9(A) shows enhanced (∼2.0-fold and ∼1.6-fold respectively) amplifications of a 1035 bp Hspa1a promoter DNA fragment from the human genomic DNA in the presence of 0.4 and 0.8 nM rutile TiO_2 nanoparticles. Similarly, rutile nanoparticles also augmented (by ∼2.2-fold) the amplification of a 364 bp HMGCR Exon 11 DNA fragment from mouse genomic DNA (figure 9(B)). Thus, rutile nanoparticles were effective for enhancement in the PCR amplification of a variety of amplicons, including the long (1035 bp) and high (60.1%) GC content human Hspa1a promoter as well as the short (364 bp) and low (51.9%) GC content mouse HMGCR Exon 11 PCR products (figures 9(A) and (B)). Notably, under identical reaction conditions, no significant difference in the PCR-enhancing effect between the rutile and anatase nanoparticles was observed (figures 9(B) and (C)), suggesting the effectiveness of both types of TiO_2 nanoparticles.

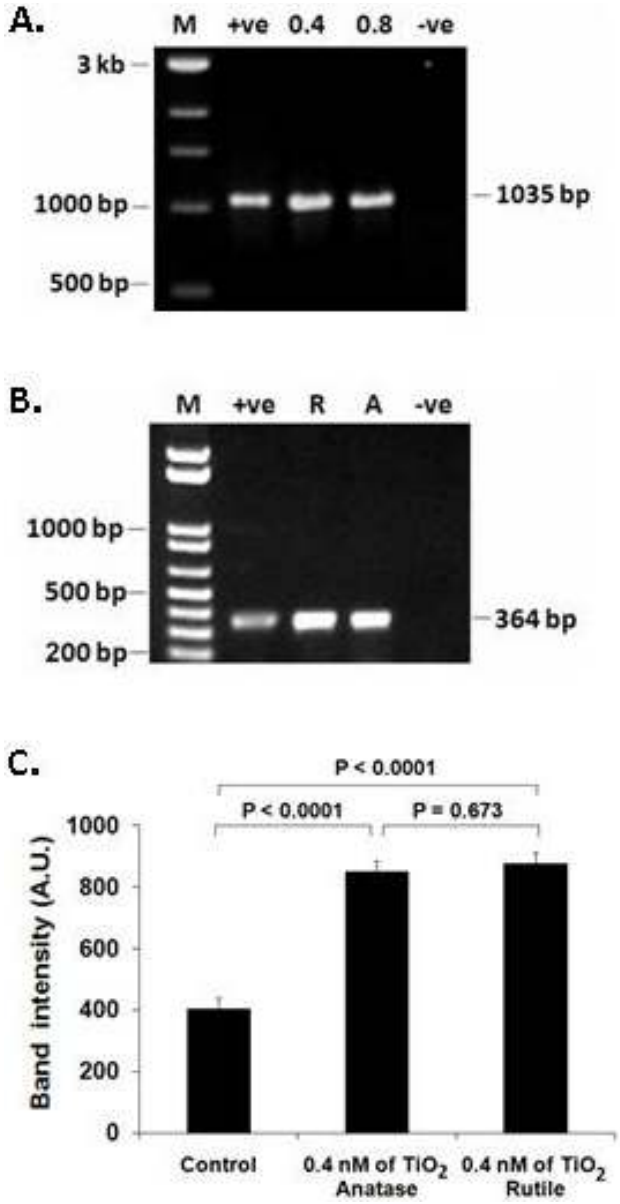

Figure 9. PCR enhancement by rutile TiO_2 nanoparticles. (A) Agarose gel electrophoresis of PCR products showing the enhancing effect of rutile TiO_2 nanoparticles. PCR amplification of a 1035 bp region of human HSPA1A promoter was carried out in the presence of 0.4 and 0.8 nM rutile TiO_2 nanoparticles. The lane labeled as '+ve' indicates the PCR products obtained under identical conditions without the addition of the nanoparticles and the lane labeled as '−ve' indicates the negative control reaction in which water was added instead of template DNA. The lane labeled as 'M' shows positions of the DNA molecular weight markers. (B) Comparison of the effectiveness between anatase and rutile nanoparticles. PCR was carried out using 0.4 nM of rutile (lane R) or anatase (lane A) nanoparticles or without any nanoparticles (+ve) to amplify a 364 bp mouse HMG-CoA reductase gene fragment. The rutile and anatase nanoparticles displayed ∼2.2-fold and ∼2.0-fold enhancement of PCR yield with respect to the control. The lane labeled as '−ve' indicates the negative control reaction in which water was added instead of template DNA. (C) Quantitative estimation of relative amounts of PCR yields. The 364 bp amplicon was PCR amplified in the presence or absence of 0.4 nM anatase or rutile nanoparticles. Results from triplicate experiments were analyzed by densitometry and plotted. No difference ($p = 0.673$) in the PCR-enhancing effect between similar sized rutile and anatase nanoparticles was observed. A.U.: arbitrary unit.

4. Conclusions and perspectives

Although PCR has become a fundamental technique in molecular biology, there is scope for further improvements to broaden its applicability in routine diagnostics, to enhance the specificity and efficiency of the amplified products as well as to minimize the costs for high-throughput applications. In view of some recent studies on enhancement of PCR by various nanoparticles, we tested the effect of TiO_2 nanoparticles in PCR in this study. Moreover, we explored the mechanism that may underlie nanoparticle-assisted PCR because this has not been systematically investigated in the previous studies.

We observed that TiO_2 nanoparticles increase the PCR yield in a concentration-dependent manner, with maximal augmentation up to 6.9-fold at 0.4 nM. Importantly, these nanoparticles were effective in enhancing the PCR efficiency for various amplicons having (i) low (46%) as well as high GC content (as much as 66.3%), (ii) different sizes (from as low as ∼364 bp to as high as ∼1035 bp). The enhancing effect was also consistently observed in different types of templates: human and mouse genomic DNA, plasmid DNA as well as mouse cDNA. Besides significant increases in PCR yield, TiO_2 nanoparticles also displayed excellent efficiency in reducing the PCR reaction time to a great extent. Indeed, as much 50% reduction in PCR run time could be achieved by these nanoparticles without compromising with the amount of amplification. Of note, the PCR-enhancing effect of TiO_2 nanoparticles was observed for both anatase and rutile polymorphic forms of TiO_2 and the extents of increments in the PCR efficiency were similar for both these polymorphs.

What might be the mechanism for enhancement of PCR efficiency by TiO_2 nanoparticles? Prior studies documenting significant improvements of both the specificity and sensitivity of PCR reactions by gold nanoparticles [19, 26, 27] have not unraveled the exact mechanisms. However, enhanced heat conductivity was thought to be responsible in view of the high thermal efficiency and thermal conductivity of gold nanoparticle-suspensions in water [8, 9]. It was also suggested that the selective interaction of gold particles and single-stranded DNA could minimize mispairing between primers and templates, enhancing the specificity and yield of PCR product [26]. A similar phenomenon may also occur in the case of TiO_2 nanoparticles. Our simulation data showed that TiO_2 nanoparticles were capable of conducting heat through the base fluid much faster than the fluid without nanoparticles. Furthermore, we observed that these nanoparticles increase the extent of denaturation of genomic DNA. Because denaturation of double-stranded DNA is the very first step of the PCR amplification process, an efficient denaturation in the presence of TiO_2 nanoparticles would improve the PCR performance. As our UV-spectroscopic measurements indicated the existence of DNA–TiO_2 nanoparticle interaction at temperatures as low as 35 °C, it is conceivable that DNA may undergo denaturation at the nanoparticle surface initially (perhaps by some catalytic mechanism) and this denaturation process is augmented at higher temperatures.

In summary, to the best of our knowledge, this study shows for the first time a significant improvement of PCR efficiency by TiO_2 nanoparticles. We have demonstrated that these nanoparticles not only enhance the amount of PCR product, they also enable reduction of the number of cycles and the time-span of the cycles without compromising the PCR yield. Both Fluent K epsilon turbulent modeling data and DNA denaturation data suggest that such an improvement in PCR is mediated by the excellent heat transfer property of these nanoparticles. The strategy of TiO_2 nanoparticle-assisted PCR may be useful for profound reduction of the overall PCR reaction period and for the amplification of difficult-to-amplify DNA templates (such as mammalian promoter sequences that often contain highly GC-rich regions).

Acknowledgments

The first author of this article expresses his sincere gratitude to Professor Amjad Ahmed Syed, Dr Sahul Hameed A S, the management of C Abdul Hakeem College of Engineering and Technology, Melvisharam for their persistent encouragement and support, and Professor M S Shaila, Indian Institute of Science Bangalore for her help in the early phase of this study. The authors thank Dr B U Nair, CLRI, Chennai and A K Samal, Department of Chemistry, IIT Madras for their help in carrying out the DNA denaturation and x-ray diffraction experiments, respectively.

This study was supported by grants from the Industrial Consultancy & Sponsored Research at IIT Madras, Department of Biotechnology and Council of Scientific & Industrial Research, Government of India. Equipment support was provided by the Department of Science and Technology, Government of India.

References

[1] Ausubel F M, Brent R, Kingston R E, Moore D D, Seidman J G, Smith J A and Struhl K 1999 *Current Protocols in Molecular Biology* (New York: Wiley)

[2] Chakrabarti R and Schutt C E 2001 The enhancement of PCR amplification by low molecular-weight sulfones *Gene* **274** 293

[3] Sarkar G, Kapelner S and Sommer S S 1990 Formamide can dramatically improve the specificity of PCR *Nucleic Acids Res.* **18** 7465

[4] Henke W, Herdel K, Jung K, Schnorr D and Loening S A 1997 Betaine improves the PCR amplification of GC-rich DNA sequences *Nucleic Acids Res.* **25** 3957

[5] Ralser M, Querfurth R, Warnatz H J, Lehrach H, Yaspo M L and Krobitsch S 2006 An efficient and economic enhancer mix for PCR *Biochem. Biophys. Res. Commun.* **347** 747

[6] Nagai M, Yoshida A and Sato N 1998 Additive effects of bovine serum albumin, dithiothreitol, and glycerol on PCR *Biochem. Mol. Biol. Int.* **44** 157

[7] Liu W T 2006 Nanoparticles and their biological and environmental applications *J. Biosci. Bioeng.* **102** 1

[8] Keblinski P, Phillpot S R, Choi S S and Eastman J A 2002 Mechanisms of heat flow in suspensions of nano-sized particles (nanofluids) *Int. J. Heat Mass Transfer* **45** 855

[9] Hu M and Gregory H V 2002 Heat dissipation for Au particles in aqueous solution: relaxation time versus size *J. Phys. Chem.* B **106** 7029

[10] Zhang J Z 1997 Ultrafast studies of electron dynamics in semiconductor and metal colloidal nanoparticles: effects of size and surface *Acc. Chem. Res.* **30** 423

[11] Das S K, Choi S U S, Yu W and Pradeep T 2007 *Nanofluids: Science and Technology* (New Jersey: Wiley)

[12] Choi S U S and Eastman J A 1995 *1995 Int. Mechanical Engineering Congress and Exhibition (San Francisco, CA)*
[13] Das S K, Choi S U S and Patel H E 2006 Heat transfer in nanofluids—a review *Heat Transfer Eng.* **27** 3
[14] Das S K, Putra N, Thiesen P and Roetzel W 2003 Temperature dependence of thermal conductivity enhancement for nanofluids *J. Heat Transfer* **125** 567
[15] Xuan Y, Li Q and Hu W 2002 Aggregation structure and thermal conductivity of nanofluids *AIChE J.* **49** 1038
[16] Link S, Burda C, Wang Z L and El-Sayed M A 1999 Electron dynamics in gold and gold–silver alloy nanoparticles: the influence of a nonequilibrium electron distribution and the size dependence of the electron–phonon relaxation *J. Chem. Phys.* **111** 1255
[17] Patel H E, Das S K, Sundararajan T, Nair S A, George B and Pradeep T 2003 Thermal conductivities of naked and monolayer protected metal nanoparticle based nanofluids: manifestation of anomalous enhancement and chemical effects *Appl. Phys. Lett.* **83** 2931
[18] Kumar D H, Patel H E, Kumar V R R, Sundararajan T, Pradeep T and Das S K 2004 Model for heat conduction in nanofluids *Phys. Rev. Lett.* **93** 144301
[19] Li M, Lin Y C, Wu C C and Liu H S 2005 Enhancing the efficiency of a PCR using gold nanoparticles *Nucleic Acids Res.* **33** e184
[20] Zhang Z, Wang M and An H 2007 An aqueous suspension of carbon nanopowder enhances the efficiency of a polymerase chain reaction *Nanotechnology* **18** 355706
[21] Nie L, Gao L, Yan X and Wang T 2007 Functionalized tetrapod-like ZnO nanostructures for plasmid DNA purification, polymerase chain reaction and delivery *Nanotechnology* **18** 015101
[22] Murshed S M S, Leong K C and Yanga C 2005 Enhanced thermal conductivity of TiO_2-water based nanofluids *Int. J. Therm. Sci.* **44** 367
[23] Wong C, Mahapatra N R, Chitbangonsyn S, Mahboubi P, Mahata M, Mahata S K and O'Connor D T 2003 The angiotensin II receptor (Agtr1a): functional regulatory polymorphisms in a locus genetically linked to blood pressure variation in the mouse *Physiol. Genomics* **14** 83
[24] Yu W, France D M, Routbort J L and Choi S U S 2008 Review and comparison of nanofluid thermal conductivity and heat transfer enhancements *Heat Transfer Eng.* **29** 432
[25] Li S Q, Zhu H, Zhu R R, Sun X Y, Yao S D and Wang S L 2008 Impact and mechanism of TiO_2 nanoparticles on DNA synthesis *in vitro Sci. China* B **51** 367
[26] Li H, Huang J, Junhong L, An H, Zhang X, Zhang Z, Fan C and Hu J 2005 Nanoparticle PCR: nanogold-assisted PCR with enhanced specificity *Angew. Chem. Int. Edn* **44** 5100
[27] Huang S-H, Yang T-C, Tsai M-H, Tsai I-S, Lu H-C, Chuang P-H, Wan L, Lin Y-J, Lai C-H and Lin C-W 2008 Gold nanoparticle-based RT-PCR and real-time quantitative RT-PCR assays for detection of Japanese encephalitis virus *Nanotechnology* **19** 405101